Journal Name

COMMUNICATION

On the dual reactivity of a Janus-type mesoionic dipole: experiments and theoretical validation

Received 00th January 20xx,
Accepted 00th January 20xx

DOI: 10.1039/x0xx00000x

www.rsc.org/

Juan García de la Concepción,[a,*] Martín Ávalos,[a] Pedro Cintas,[a,*] José L. Jiménez,[a] and Mark E. Light[b]

A mesoionic bicycle, easily synthesized from a proteinogenic amino acid, L-leucine, behaves as both thiazolium-olate and diazolium-olate dipoles, as unveiled by its dipolar cycloadditions. This chameleonic reactivity has been thoroughly interpreted by dissecting the mechanistic landscape aided by the distortion-interaction model.

The concept of dual reactivity, by which single molecules may exhibit complementary and often opposing roles, allows for elegant and divergent synthetic strategies, which would otherwise require multiple reagents or pathways. This vast concept is well exemplified by tautomeric species and umpolung effects of the classical carbonyl reactivity.[1] More recent and specific development include new catalysts with dual reactivity,[2] ambivalent reaction conditions,[3] and chameleonic behaviors shown by simple reagents like acetylenes, oximes, hydrides, and even water.[4]

Given the enormous versatility of [3+2]-cycloaddition reactions en route to highly-functionalized heterocycles present in natural products and pharmaceuticals,[5] 1,3-dipoles by virtue of their bielectronic character might be susceptible of opposing reactivities. However, to our knowledge the dipolar duality has not yet been achieved and most dipoles follow invariably well-established reactivity patterns. Among cyclic dipoles, mesoionic heterocycles were once postulated to exist in equilibrium with their uncharged valence tautomers, but trapping of such species remains largely elusive. Some alkylated 1,3-thiazolium-4-olates (dubbed thioisomünchnones), however, appear to equilibrate with non-dipolar tautomers that react as mild nucleophiles in the presence of strong electrophiles.[6]

Clearly the possibility of detecting dual reactivity hinges on dipoles prone to tautomeric equilibria. Herein we show the proof of principle with a bicyclic ring-fused thioisomünchnone (**3**), which can easily be obtained in a few steps from the naturally-occurring amino acid L-leucine (**1**), via the intermediacy of its hydantoin **2** (Figure 1, top).[7] Compound **3** shows the expected masked dipole at the C2-S1-C8 fragment, namely a 1,4-thiazolium-3-olate. Proton transfer, however, from C5 to C2 would render a different mesoionic ring (**4**: 4,7-diazolium-6-olate; Figure 1, middle), where the masked dipole is now located across the C5-N4-C8 bonds. This kind of dipoles has received little attention, although a recent study has demonstrated its synthetic utility by reaction with acetylenes.[8] The unequivocal identity of **3** can be inferred from its spectroscopic data. In particular, a triplet signal resonating at 5.03 ppm can be reliably assigned to the hydrogen atom at the C5 atom (see ESI). Clearly, the term "Janus" (i.e. "two faces") is appropriate and eye-catching to denote the dual reactivity of this mesoionic heterocycle. A dipolarophile could intercept either of them (**3** and **4**), so long as such dipoles equilibrate in solution. To check this surmise, compound **3** was reacted with two representative and reactive alkenes, such as 1-phenyl-1*H*-pyrrole-2,5-dione (**5**) and dimethyl (*E*)-butenedioate (**6**). These cycloadditions were heated in toluene using a professional MW oven (2.45 GHz), thereby enabling accurate control of both power and temperature (see ESI) for 1h. Although complex mixtures were detected by TLC analyses, the resulting products evolving from the dipolar cycloaddition could be isolated by crystallization (diethyl ether) from the reaction mixture. The dipolar cycloaddition of **3** with **5** gave rise to the *endo* cycloadduct **7** in 45% yield. Gratifyingly, crystals of the latter suitable for X-ray diffraction were grown by slow evaporation and allowed us its unequivocal structural elucidation (Figure 1, bottom). In a previous study, it has been shown the marked facial control exerted by a bulky alkyl group in the dipole,[9] a fact corroborated by the present result as well. The cycloaddition with **6** was likewise conducted as described above and a different dihydropyrrole structure (**8**) could be isolated in 24% yield. Both NMR (showing the lack of a CH_4O fragment) and elemental analysis were inconsistent with the expected cycloadduct (with molecular formula $C_{27}H_{26}N_2O_6S$). Again, X-ray diffractometry was rewarding enough to confirm the unambiguous solid-state structure of **8** (Figure 1, bottom). The formation of the latter cannot be rationalized if one assumes the cycloaddition of **6** with a 1,4-thiazolium-3-olate moiety, but rather with its chameleonic transformation into 4,7-diazolium-6-olate. Scheme 1 outlines a mechanistic proposal, where

[a] Departamento de Química Orgánica e Inorgánica. Facultad de Ciencias-UEX. IACYS-Unidad de Química Verde y Desarrollo Sostenible. E-06006 Badajoz (Spain). E-mail: jugarco@unex.es. Fax: (+34) 924-271-149
[b] Department of Chemistry. University of Southampton. Southampton SO17 1BJ, U.K.

† Electronic Supplementary Information (ESI) available: X-ray diffraction analysis, copies of NMR spectra of all synthetic products and cartesian coordinates for all optimized geometries. See DOI: 10.1039/x0xx00000x

the formation of **8** would proceed through the generation of cycloadduct **9** by a ring-opening pathway that we shall discuss in detail later.

To understand the differential reactivity of dipoles **3** and **4** against compounds **5** and **6**, we performed a full computational study at the ONIOM(M06-2X/6-311++G(d,p):M06-2X/6-31G) level of theory[10-12] using the Gaussian09 package.[13] Furthermore, to reproduce the experimental conditions, all calculations were carried out in toluene (SMD model)[14] at 373.1 K. A distortion/interaction (D/I) model was employed to assess the origin of the reactivity of the dipolar cycloadditions. The D/I model has proven to be a useful tool to predict and justify the reactivity of mesoionic dipoles.[15,16] Figure 2 shows the optimized geometries of the reactants where the ball and wireframe representations correspond to high- and low-level calculations, respectively. In addition and, given the inherent chirality provided by L-leucine, the formation of all the possible diastereomers during the approaches of **5** (or **6**) to dipoles **3** and **4** were taken into consideration as well. This analysis affords up to four cycloadducts from each pair of reactants. Although the mesoionization protocol resulted in extensive racemization yielding compounds **3** and **4** as essentially racemic mixtures, the remaining computation focused on the (*R*)-configured enantiomer to assess

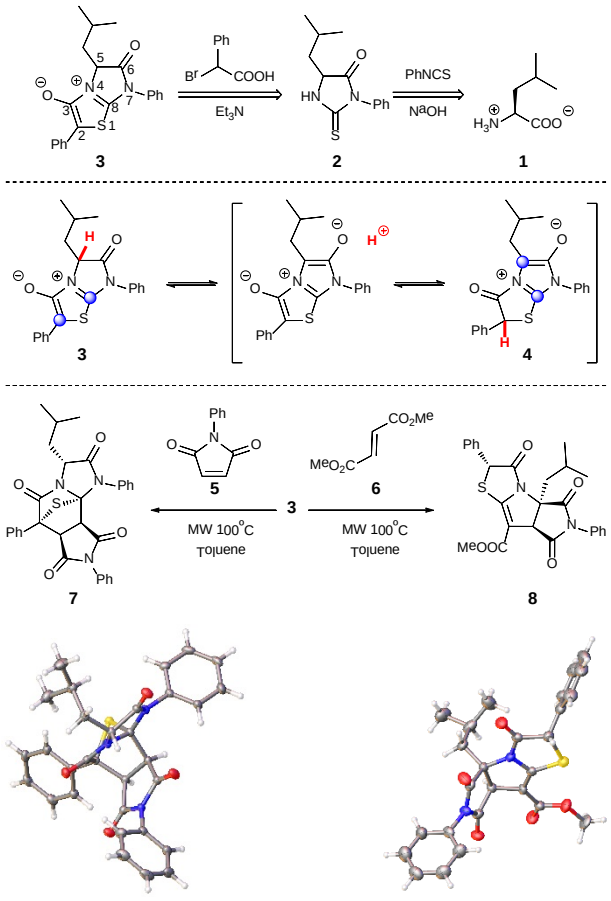

Figure 1. Retrosynthetic route for the preparation of 5-isobutyl-6-oxo-2,7-diphenyl-6,7-dihydro-5*H*-imidazo[2,1-*b*]thiazol-4-ium-3-olate (**3**) (top). Equilibrium between mesoionic heterocycles **3** and **4** (middle). Reactions of thioisomünchnone **3** with dipolarophiles 5 and **6** leading to the *endo* cycloadduct **7** and dihydropyrrole **8**, respectively. X-ray structures of **6** (left) and **7** (right) shown at 50% ellipsoid probability (bottom).

the facial stereocontrol exerted by both the isobutyl group of **3** and the phenyl group of **4**. It is noteworthy the greater relative stability of dipole **3** with respect to **4** by 6.7 kcal mol^{-1}. A topological analysis of electron density[17] of both mesoionic rings show very similar results electron density [ρ(r)] and Laplacian of the electron density [$\nabla^2\rho(r)$] in their five bond critical points (BCP) and ring critical points (RCP), which point to similar reactivity as dipoles (see ESI).

Figures 3 and 4 show the computed reaction pathways for dipolarophiles **5** and **6** *versus* dipoles **3** (top) and **4** (bottom). The energy barriers for the reactions between **4** and **5** are lower than those estimated for the cycloadditions with the thiazolium-olate dipole (**3**). The enhanced reactivity of the diazolium-olate tautomer (**4**) is consistent with a higher interaction energy wit compound **5** (see Figure 5, top).

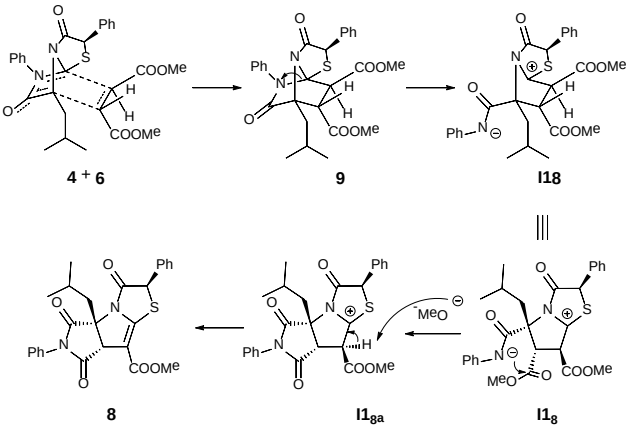

Scheme 1. Tentative mechanism for the formation of **8**.

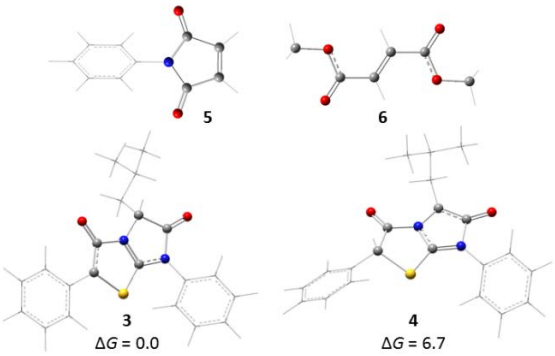

Figure 2. Optimized geometries of dipoles **3** and **4** and dipolarophiles **5** and **6** at the ONIOM(M06-2X/6-311++G(d,p):M06-2X/6-31G) level of theory in toluene (SMD) at 373.1 K. Ball and wireframe representations correspond to high- and low-level calculations, respectively. Relative free energy values of **3** and **4** are given in kcal mol^{-1}.

The less favored approaches of **3** to **5** correspond to the formation of *exo* cycloadducts **10** and **11**. The geometries of the corresponding saddle points **TS1$_{11}$** and **TS$_{10}$** are quite similar, and although the formation of **11** proceeds by a stepwise process, the structure of **TS$_{10}$** is characteristic of a very asynchronous cycloaddition. Both saddle points (**TS1$_{11}$** and **TS$_{10}$**) shows a pronounced steric hindrance caused by the phenyl group linked to N7 in dipole **3**, which prevents close contacts between dipole and dipolarophile (Figure 6) which translates into a high distortion energy of the dipolarophile.

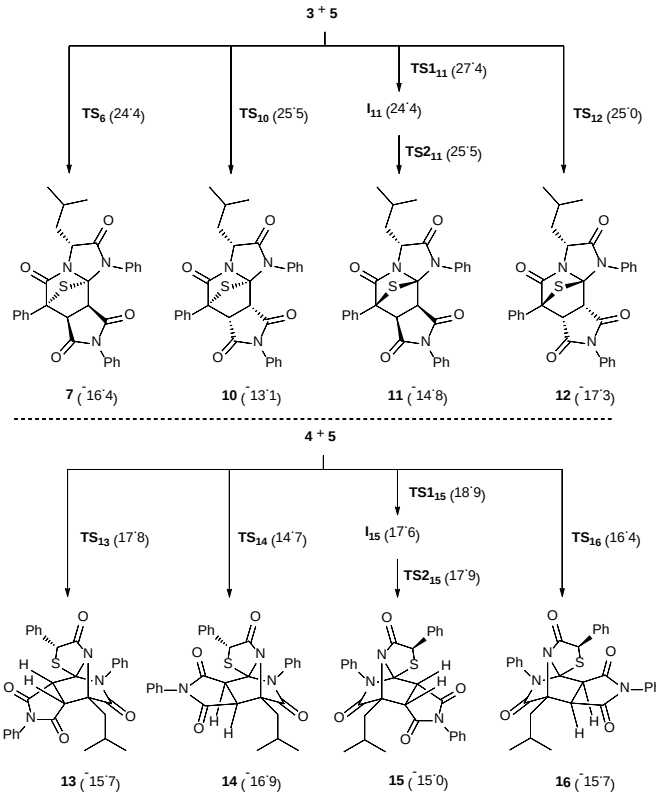

Figure 3. Computed free energy barriers for the reaction of dipolarophile 5 with dipoles 3 (above) and 4 (below) at the ONIOM(M06-2X/6-311++G(d,p):M06-2X/6-31G) level, in toluene (SMD) at 373.1 K. Energy values are given in kcal mol^{-1}.

Likewise, the less favored cycloadditions of **5** with the diazolium-olate (**4**) correspond to either stepwise (**TS1$_{15}$**) or asynchronous (**TS$_{13}$**) cycloadditions, which lead however to *endo* cycloadducts **13** and **15**. The phenyl group at the N7 position exhibits a strong π-π stacking interaction with the phenyl group of **4**.

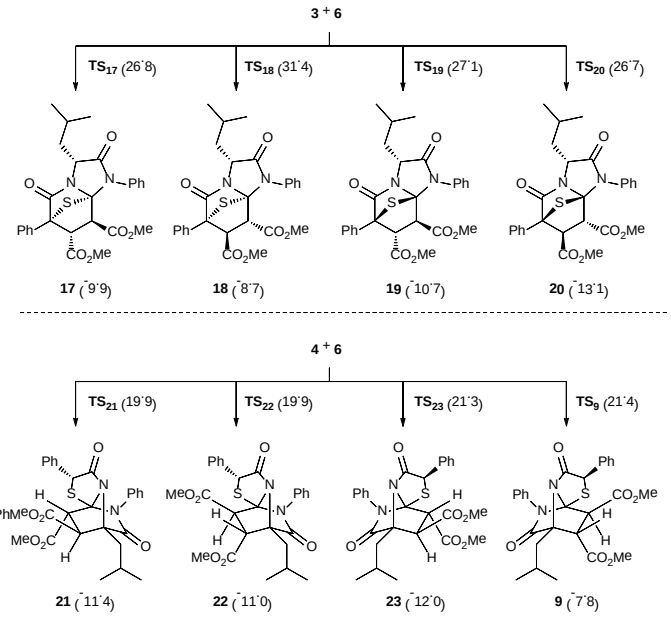

Figure 4. Computed free energy barriers for the reaction of dipolarophile **6** with dipoles **3** (above) and **4** (below) at the ONIOM(M06-2X/6-311++G(d,p):M06-2X/6-31G) level, in toluene (SMD) at 373.1 K. Energy values are given in kcal mol^{-1}.

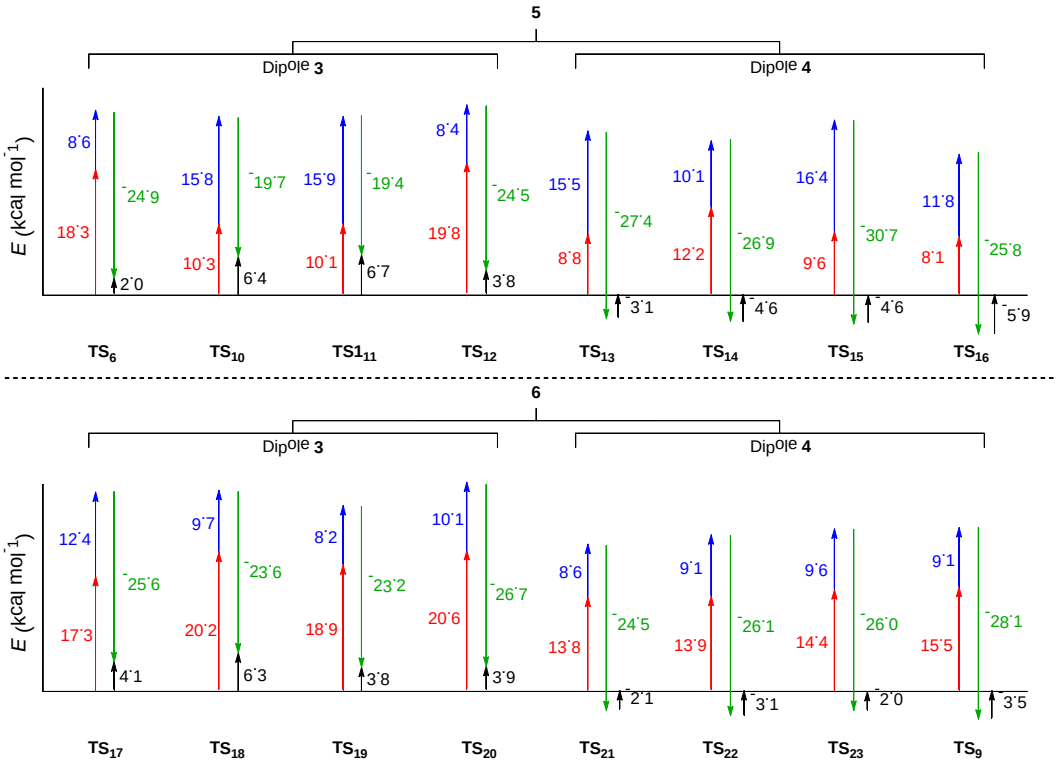

Figure 5. Distortion energies of dipoles (red), dipolarophiles (blue), interaction energies (green) and activation energies (black) for the reactions of dipoles **3** and **4** with dipolarophiles **5** (top) and **6** (bottom).

Journal Name

COMMUNICATION

Once again, such an interaction moves the dipolarophile away moiety from the dipole moiety (Figure 6), thus increasing the distortion energy of the dipolarophile.

In following the above-mentioned computational procedure, the free energy b arriers for the reaction channels of **6** to dipoles **3** and **4** are collected in Figure 4. All the approaches of **6** to the diazolium-olate dipole (**4**) show very similar energy barriers, albeit slightly higher for the saddle points involving the approach of **6** to the 5-*Si*,8-*Si* face of **4** (**TS_{23}** and **TS_9**), which show in that case a little increase in distortion energy of the dipole (Figure 5, bottom).

As mentioned, the product isolated by reaction of **4** and **6**, i.e. dihydropyrrole **8**, arises from cycloadduct **9**, whose formation is not favored, from both kinetic and thermodynamic viewpoints. These data support the complex reaction mixture obtained experimentally.

On the other hand, the reaction with the thiazolium-olate dipole (**3**) suggests that formation of cycloadduct **18** is strongly disfavored with respect to those of **17**, **19** and **20**. The corresponding saddle point that led to that cycloadduct (**TS_{18}**) shows a high total distortion energy and a low interaction energy, as expected, the phenyl group linked to the N7 atom in **3** hinders sterically one of the methyl carboxylate fragments of **6** (Figure 7). Like the cycloadditions with **5**, the results obtained for **6** point clearly to an enhanced reactivity of the diazolium-olate dipole relative to its thiazolium-olate counterpart. However, in this case, the increased reactivity is associated with a lower distortion energy of the dipole. This difference accounting for the dual reactivity of dipoles **3** and **4** with **5** and **6** does also suggest a significant influence of the structure of dipolarophiles on the energetic profile.

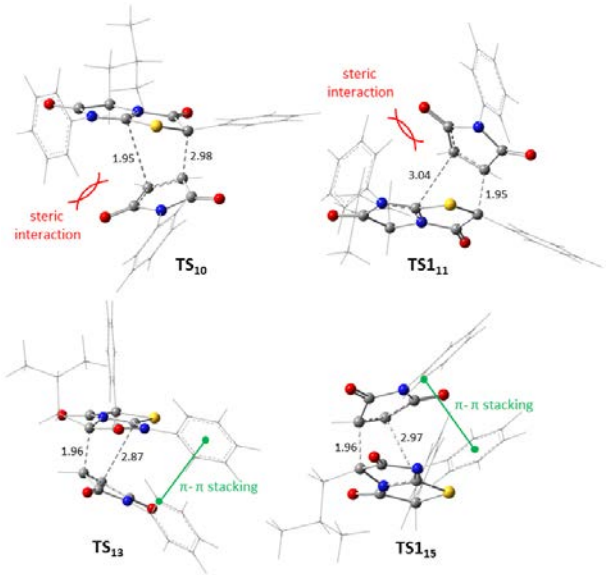

Figure 6. Optimized geometries of **TS_{10}**, **$TS1_{11}$**, **TS_{13}** and **$TS1_{15}$** at the ONIOM(M06-2X/6-311++G(d,p):M06-2X/6-31G) level of theory in toluene (SMD) at 373.1 K.

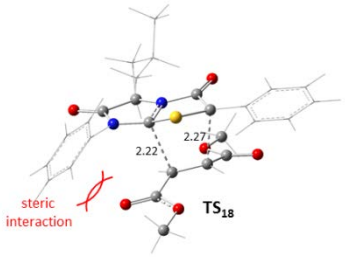

Figure 7. Optimized geometry of **TS_{18}** at the ONIOM(M06-2X/6-311++G(d,p):M06-2X/6-31G) level of theory in toluene (SMD) at 373.1 K.

Figure 8 shows the calculated reaction pathway leading to **8** via the intermediacy of cycloadduct **9**. Fragmentation of the latter alleviates ring strain yielding **$I1_8$** through the corresponding saddle point **$TS1_8$**. This kind of ring opening has been previously described for reactions of thioisomünchnones with alkenes.[18] This path would then be followed by attack of the nitrogen atom in zwitterionic intermediate **$I1_8$** to the methyl carboxylate group (**$TS2_8$**) giving rise to a tetrahedral intermediate (**$I2_8$**). The latter evolves directly to a neutral and stable intermediate (**$I3_8$**). In this transition state (**$TS3_8$**), the leaving group (methoxide) attacks directly to the carbonium ion and both bond breaking at the pyrrolidinedione ring and bond-forming step occur in a concerted manner. Lastly, **$TS4_8$** corresponds to the concerted elimination of methanol giving product **8**. The free energy profile of this elimination is consistent with a high thermodynamic control during the conversion of cycloadduct **9** into **8**.

Moreover, this computational study shows that the reactions of dipoles **3** and **4** with **5** are controlled by the dipolarophile distortion, caused to a significant extent by the phenyl group linked to N7 of the dipole, which exerts both π-π stacking and steric interactions with **5**. The stereochemical outcome with **6** depends however on the dipole. Thus, the less favored cycloaddition with dipole **3** combines high total distortion energy plus low interaction energy, while the reaction with **4** is controlled by the distortion of the dipole. In a nutshell, dipole **4** appears to be more reactive than **3**, as inferred from a higher interaction energy with the dipolarophiles evaluated. In addition, all the cycloaddition reactions of compound **5** are thermodynamically favored with respect to those of **6** (see Figures 3 and 4). Finally, the cycloadduct (**9**) that evolves into dihydropyrrole **8** is the most unstable species formed in the reaction between **4** and **6**. A further look at the reaction profile depicted in Figure 8 also indicates that the formation of **8** is largely driven by thermodynamically control.

Journal Name

COMMUNICATION

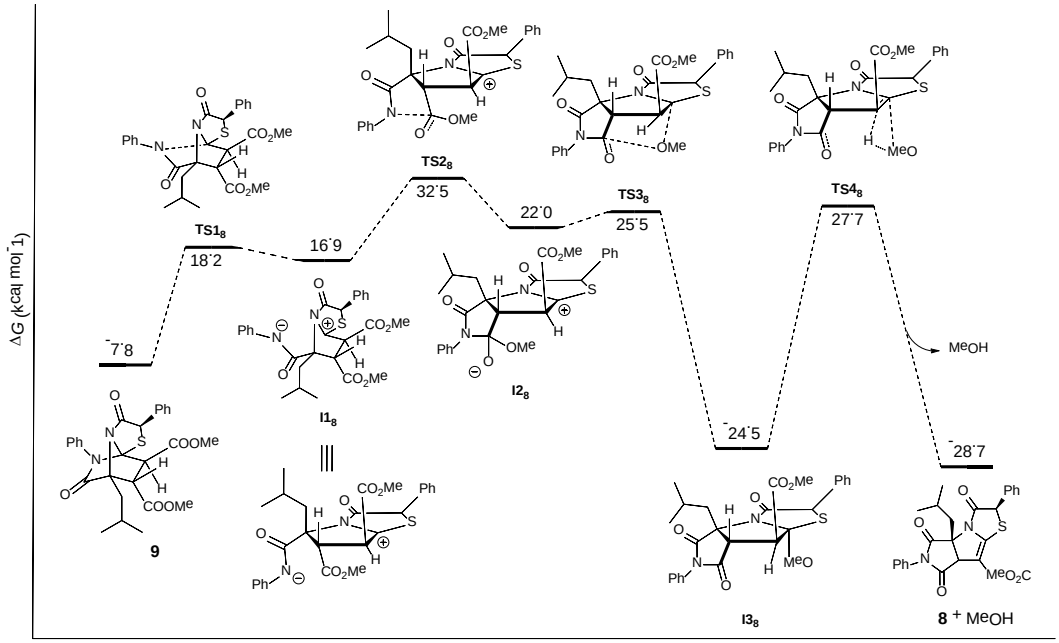

Figure 8. Reaction pathway leading to dihydropyrrole **8** from cycloadduct **9**. Free energy values are given in kcal mol^{-1}.

Conclusions

In conclusion, we disclose for the first time the anomalous behavior of a Janus-type mesoionic dipole susceptible of dual reactivity owing to proton transfer between two atom positions, giving access to divergent structures. Although this ditopic character has been shown against a couple of dipolarophiles, these preliminary results have been explained by theoretical calculations and the principle can be exploited to fine-tune the dipoles to further the scope of novel [3+2] cycloadditions.

Conflicts of interest

There are no conflicts to declare.

Notes and references

(1) (a) *Tautomerism: Concepts and Applications In Science and Technology*, ed. L. Antonov, Wiley-VCH, Weinheim, 2016. (b) R. Brehme, D. Enders, R. Fernandez and J. M. Lassaletta, *Eur. J. Org. Chem.*, 2007, 5629-5660. (c) F. Tanaka and C. F. Barbas, III, in *Enantioselective Organocatalysis: Reactions and Experimental Procedures*, ed. P. I. Dalko, Wiley-VCH, Weinheim, 2007, Ch. 2, pp. 19-55.

(2) (a) K. Shin, J. Ryu and S. Chang, *Org. Lett.,* 2014, **16**, 2022-2025. (b) l. M. Loftus, J. K. White, B. A. Albani, L. Kohler, J. J. Kodanco, R. P. Thummel, K. R. Dunbar and C. Turro, *Chem. Eur. J.,* 2016, **22**, 3704-3708. (c) A. Causero, H. Elsen, G. Ballmann, A. Escalona and S. Harder, *Chem. Comm*., 2017, **53**, 10386-10389. (d) A. Widera, E. Kaifer, H. Wadepohl and H.-J. Himmel, *Chem. Eur. J.,* 2018, **24**, 1209-1216.

(3) L. Buzzetty, A. Prieto, S. R. Roy and P. Melchiorre, *Angew. Chem. Int. Ed*., 2017, **56**, 15039-15043.

(4) (a) C. Izquierdo, F. Esteban, A. Parra, R. Alfaro, J. Alemán, A. Fraile and J. L. García Ruano, *J. Org. Chem*., 2014, **79**, 10417-10433. (b) B. A. Trofimov and E. Y. Schmidt, *Acc. Chem. Res*., 2018 in press (doi: 10.1021/acs.accounts.7b00618). (c) P. Merino, M. A. Chiacchio, L. Legnani, I. Delso and T. Tejero, *Org. Chem. Front*., 2017, **4**, 1541-1554. (d) Y. Mao, Y. Liu, Y. Hu, L. Wang. S. Zhang and W. Wang, *ACS Catal*., 2018, **8**, 3016-3020. (e) S. Sadhukhan and B. Baire, *Adv. Synth. Catal.,* 2018, **360**, 298-304.

(5) (a) *Synthetic Applications of 1,3-Dipolar Cycloaddition Toward Heterocycles and Natural Products*, eds. A. Padwa and W. F. Pearson, John Wiley & Sons, New York, 2002. (b) H. Pellisier, *Tetrahedron,* 2007, **63**, 3235-3285. (c) H. Suga and K. Itoh, in *Methods and Applications of Cycloaddition Reactions in Organic Synthesis*, ed. N. Nishiwaki, John Wiley & Sons, Hoboken, NJ, 2013, pp. 175-204.

(6) M. Ávalos, R. Babiano, P. Cintas, J. Díaz, J. L. Jiménez, I. López and J. C. Palacios, *Eur. J. Org. Chem.*, 2004, 2805-2811.

(7) (a) D. M. Wolfe and P. R. Schreiner, *Synthesis*, 2007, **13**, 2002-2008. (b) G. S. M. Sundaram, C. Venkatesh, H. Ila and H. Junjappa, *Synlett*, 2007, **2**, 251-254.
(8) H, Erguven, D. C. Leitch, E. N. Keyzer, B. A. Arndtsen, *Angew. Chem. Int. Ed.* 2017, **56**, 6078-6082.
(9) J. García de la Concepción, M. Ávalos, P. Cintas, J. L. Jiménez and M. E. Light *Org. Biomol. Chem*., 2018, **16**, 3438-3452.
(10) (a) S. Dapprich, I. Komáromi, K. S. Byun, K. Morokuma and M. J. Frisch, *J. Mol. Struct. (Theochem),* 1999, **461-462**, 1-21. (b) F. Maseras and K. Morokuma, *J. Comp. Chem.*, 1995, **16**, 1170-1179. (c) R. D. Froese and K. Morokuma, in *The Encyclopedia of Computational Chemistry,* eds. P. v. R. Schleyer, N. L. Allinger, T. Clark, J. Gasteiger, P. A. Kollman, H. F. Schaefer, III and P. R. Schreiner, John Wiley & Sons, Chichester, 1998, pp. 167-183.
(11) (a) Y. Zhao and D. G. Truhlar, *Theor. Chem. Acc*., 2008, **120**, 215-241. (b) Y. Zhao and D. G. Truhlar, *Acc. Chem. Res*., 2008, **41**, 157-167.
(12) (a) R. Ditchfield, W. J. Hehre and J. A. Pople, *J. Chem. Phys*., 1971, **54**, 724–728. (b) W. J. Hehre, R. Ditchfield and J. Pople, A. *Mol. Phys*., 1974, **27**, 209–214. (c) M. S. Gordon, *Chem. Phys. Lett*., 1980, **76**, 163–168. (d) P. C. Hariharan and J. A. Pople, *Theor. Chem. Acc*., 1973, **28**, 213–222. (e) M. M. Francl, W. J. Pietro, W. J. Hehre, J. S. Binkley, D. J. DeFrees, J. A. Pople and M. S. Gordon, *J. Chem. Phys*., 1982, **77**, 3654–3665.
(13) M. J. Frisch, G. W. Trucks, H. B. Schlegel, G. E. Scuseria, M. A. Robb, J. R. Cheeseman, G. Scalmani, V. Barone, B. Mennucci, G. A. Petersson, H. Nakatsuji, M. Caricato, X. Li, H. P. Hratchian, A. F. Izmaylov, J. Bloino, G. Zheng, J. L. Sonnenberg, M. Hada, M. Ehara, K. Toyota, R. Fukuda, J. Hasegawa, M. Ishida, T. Nakajima, Y. Honda, O. Kitao, H. Nakai, T. Vreven, Jr., J. A. Montgomery, J. E. Peralta, F. Ogliaro, M. Bearpark, J. J. Heyd, E. Brothers, N. K. Kudin, V. N. Staroverov, R. Kobayashi, J. Normand, K. Raghavachari, A. Rendell, J. C. Burant, S. S. Iyengar, J. Tomasi, M. Cossi, N. Rega, J. M. Millam, M. Klene, J. E. Knox, J. B. Cross, V. Bakken, C. Adamo, J. Jaramillo, R. Gomperts, R. E. Stratmann, O. Yazyev, A. J. Austin, R. Cammi, C. Pomelli, J. W. Ochterski, R. L. Martin, K. Morokuma, V. G. Zakrzewski, G. A. Voth, P. Salvador, J. J. Dannenberg, S. Dapprich, A. D. Daniels, Ö Farkas, J.B. Foresman, J. V. Ortiz, J. Cioslowski and D. J. Fox, Gaussian 09, Revision D.01, Gaussian, Inc., Wallingford, CT, 2009.
(14) A. V. Marenich, C. J. Cramer and D. G. Truhlar, *J. Phys. Chem. B*, 2009, **113**, 6378-6396.
(15) M. Ávalos, R. Babiano, J. L. Bravo, P. Cintas, J. L. Jiménez, J. C. Palacios and Silva, M. A. *J. Org. Chem*., 2000, **65**, 6613-6619.
(16) K. N. Houk and P. A. Champagne, *J. Org. Chem*., 2017, **82**, 10980-10988.
(17) R. F. W. Bader, *Atoms in Molecules: A Quantum Theory*, Oxford University Press, Oxford, 1990.
(18) M. Ávalos, R. Babiano, A. Cabanillas, P. Cintas, F. J. Higes, J. L. Jiménez and J. C. Palacios, *J. Org. Chem*., 1996, **61**, 3738-3748.

